Journal of Engineering Science and Technology
Vol. 18, No. 2 (2023) 1323 - 1338

EFFECT OF HEAT TREATMENT CYCLES ON TENSILE PERFORMANCE AND MICROSTRUCTURAL EVOLUTION OF THIXOFORMED MWCNT-A356 COMPOSITE

H. HANIZAM[1,*], M. S. SALLEH[2], Z. MARJOM[1], M. Z. OMAR[3], A. B. SULONG[3], S. A. SUNDI[1], H. BOEJANG[1], A. H. ABDUL RASIB[1]

[1]Fakulti Teknologi Kejuruteraan Mekanikal dan Pembuatan, Universiti Teknikal Malaysia Melaka, Hang Tuah Jaya, 76100 Durian Tunggal, Melaka, Malaysia
[2]Fakulti Kejuruteraan Pembuatan, Universiti Teknikal Malaysia Melaka, Hang Tuah Jaya, 76100 Durian Tunggal, Melaka, Malaysia
[3]Department of Mechanical and Materials Engineering, Faculty of Engineering and Built Environment, Universiti Kebangsaan Malaysia, Bangi 43600, Malaysia
*Corresponding Author: hanizam@utem.edu.my

Abstract

A liquid casting of multi-walled carbon nanotubes (MWCNT)-A356 alloy composite is an excellent alternative in the production of automotive parts. The casting process begins by premixing the MWCNT and magnesium powder as reinforcement and wettability agent, respectively before inserted into the liquid matrix. Mechanical stirring promotes uniform distribution of MWCNT and forming the non-dendritic microstructure by convection and shearing forces. Thixoforming process was carried out at 50 % of liquid fraction followed by T5 and T6 heat treatment cycles. Composite grain structure and intermetallic phases were characterized using an optical microscope and X-ray diffraction procedures. Meanwhile, the investigations of MWCNT distribution and tubular structural integrity on tensile test fracture samples using the field-emission microscopic and Raman spectroscopy were uniformly distributed and with minimum damage. The ultimate tensile strength (UTS) of thixoformed composites after T5 and T6 were improved by 7.2% (270.5 MPa) and 30.8% (330.3 MPa), respectively. The enhancement of T6 is higher than T5, corroborating with the isothermal holding at 540 °C during the solution treatment permits the further dissolution of eutectic α-Al and precipitates, allows better distribution of MWCNT and promotes higher strengthening mechanisms.

Keywords: Aluminium alloy composite, Carbon nanotubes, Heat treatment, Tensile strength, Thixoforming.

1. Introduction

A356 hypoeutectic alloy reinforced with multi-walled carbon nanotube (A356-MWCNT) composite has a great potential to replace current aluminium alloy applications in automotive and aerospace industries [1, 2]. The A356 aluminium alloy matrix exhibits high fluidity, good castability, high strength to weight ratio and high corrosion resistance which is suitable for the production of near or net-shaped components such as wheels and suspension arms [3-5]. Currently, powder metallurgy (PM) is the most preferred method of MWCNT-aluminium composite production as the technique can overcome the limitations of obtaining a homogeneous distribution of MWCNT in the alloy matrix [6]. However, these automotive and aerospace components require high mechanical strength and often complex in shape, large in size, high in production volume, and reasonable in cost that limit the capability of PM. Although some have combined the PM with liquid casting or often called as hybrid method, full liquid casting processing is still the best-suited method [7]. Besides, PM causes severe tube structural damage of MWCNT during a ball milling mixing process resulting and reduces the optimum reinforcement strengthening potential.

In comparison with the alloy, the superior mechanical strength of the liquid casting MWCNT-A356 composite is achieved by the incorporation of just a small amount of MWCNT~0.5% by weight percentage into the A356 matrix. Enhancement of mechanical strength by the MWCNT involves mechanisms such as load transfer, Orowan looping, and thermal mismatched dislocations [8-10]. However, the high effectiveness of the mechanisms can be achieved only with uniform MWCNT distribution in the matrix and good interfacial bonding phases between MWCNT and matrix of aluminium carbide (Al_4C_3) formation [11, 12]. Moreover, a sound structural integrity of the MWCNT is also crucial to optimize the strengthening effect of the composite. Although damaged MWCNT can still provide the strengthening effects through Orowan looping and thermal mismatched dislocations, the load transfer mechanism between the matrix through MWCNT often predominates the mechanical strength enhancement [13]. Besides, the damaged or exposed carbon of MWCNT is prone to excessive Al_4C_3 in nanorod liked phase formations that can negatively impact and degrade the strength of the composite due to its natural brittleness [14, 15]. Therefore, as to maintain the pristine MWCNT tube structure is critical, the damaged level can be minimised through the liquid casting method.

Moreover, the matrix with non-dendritic microstructures for semi-solid processing can also be obtained through liquid casting. Thixotropic behaviour of the non-dendritic matrix that flows when sheared and remains solid when undisturbed makes it suitable for semi-solid of thixoforming. The non-dendritic feedstock composite reheat-up to a certain temperature with 30-50% of liquid to a solid fraction which was then forged into a mould [16, 17]. Thixoforming improves the strength of a composite by eliminating the casting defects such as micro porosity, coarsening of α-Al matrix and spheroidizing the β-Si microstructures [18].

Besides that, further application of T6 heat treatment on the cast A356 alloy to elevate its strength is already well established. The strengthening mechanisms involved during the heat treatment process includes precipitation of Mg_2Si and Al_2Cu, further coarsening of α-Al and spheroidization of β-Si [19]. However, a standard T6 requires long duration of heating process which includes solution treatment and artificial ageing. Other limitations of T6 standard heat treatment includes the

requirement of high temperature and the long production cycle that will directly impact the overall cost of the produced components [20]. Although the standard heat treatments of T4 and T5 are shorter in time and considered as cheaper, the treatments are seldom used for industrial application due to their lower overall strengths compared with the standard T6 [4]. Table 1 shows general heat treatment standards of permanent mould casting aluminium alloys according to the ASTM B-917M-01.

Table 1. Heat treatments of aluminium alloys.

Heat treatment	Solution treatment		Artificial ageing		Quenching
	Temp. (± 5 °C)	Time (hr)	Temp. (± 5 °C)	Time (hr)	Temp. (°C)
T4	510-520	2-10	Room temp.	120	-
T5	-	-	205	7-9	-
T6	525-540	8	155	2-5	60-100

Thus far, information of the effect of heat treatment cycles on the mechanical properties and microstructural evolution of MWCNT-A356 composite are scarce and remain unclear. So far, there has been little quantitative analysis of the reinforcement effects on alloy matrix composite due to the heat treatment process. Furthermore, a comparison study between T5 and T6 heat treatment effects on the composite strength will provide details on the heat treatment options to be applied in related industries for better cost effective process. Besides, further investigation on the influence of combined thixoforming and heat treatment processes on the composites will also be useful.

In this study, the objectives were to obtain tensile strength and microstructural transformation of thixoformed MWCNT-A356 alloy composite after heat treatment processes. The MWCNT-A356 composite was prepared using the liquid casting method that has been established previously [21]. The distribution of MWCNT in the matrix and the formation of the non-dendritic microstructure were produced using a mechanical stirring process with the use of a three-blade propeller at 500rpm for 10 minutes at 650°C of molten liquid temperature. Reheating of composite feedstock was carried out at 50% semi-solid liquid fraction or at 580°C before compacted into a top permanent mould. The thixoformed composites were then divided into two portions for T5 and T6 heat treatments applications. Mechanical properties and microstructural evolution of the composites were evaluated and presented.

2. Experimental procedures

2.1. Composite fabrication

The chemical composition of A356 alloy casting was determined using a PANalytical wavelength dispersive X-ray fluorescence (WDXRF) spectrometer and presented in Table 2. The MWCNT with a purity of > 88% and, internal and external diameters of 20-40nm and 5-10nm, respectively were purchased from Sigma-Aldrich, USA. Thermal gravimetric analysis (TGA) was conducted to determine the thermal stability of the MWCNT using a Mettler Toledo thermal gravimetric analyser. The overall MWCNT-A356 composite preparation process flow diagram can be referred to our previous published report [22]. Before the casting of composite, the mixture of 2g of each MWCNT and Mg powder or 0.5 overall weight percentage (0.5 wt.%) were

wrapped with aluminium foil of 0.2 mm thick. The Mg powder acts as a wettability agent between MWCNT and the matrix during the liquid mixing. Table 2 also shows the composition of elements in A356 alloy with the presence of 0.5 wt.% Mg addition. About 400g of A356 was melted in an induction furnace at 700°C to ensure complete melting and the furnace temperature was reduced to 650°C. The wrapped MWCNT and Mg were injected into the melted sample at the bottom of the crucible using a hollow stainless steel rod and a plunger. The melted samples were immediately stirred at a moderate speed of 500rpm for 10 minutes using a three-blade propeller. Vortex condition in the melted samples is crucial for uniform distribution of the MWCNT in the matrix and to promote non-dendritic microstructures development [22]. Finally, the molten composites were poured immediately into a pre-heated permanent steel mould at 150°C with a dimension of 120 mm (height) and 25 mm (diameter) to form a billet feedstock.

Table 2. Chemical composition of A356 and A356 + 0.5% of Mg alloys (by wt.%).

Alloy	Si	Cu	Mg	Mn	Zn	Fe	Ti
A356	6.543	0.196	0.222	0.049	0.101	0.238	0.219
A356 + 0.5 wt.% Mg	6.457	0.168	0.664	0.042	0.113	0.236	0.186

2.2. Thixoforming and heat treatments of composites

Thermal analysis of the alloy composite was carried out using a differential scanning calorimetry (DSC), Mettler Toledo. Fig. 1 shows the heat flow and liquid fraction of the A356 alloy during the endothermic reaction of the heating process. Two peaks of solidus and liquidus were detected at 575°C and 620°C, respectively which can be ascribed to solid to liquid phases transition and a highest knee condition at 575°C. The highest knee takes place when binary eutectic of the α-Al solid solution starts to melt which slows down the rate of liquid formation beyond the knee. Therefore, 50% liquid fraction at 580°C was selected as the semi-solid condition for thixoforming process in this study.

Figure 2 shows a schematic diagram of a T30-80 kHz thixoforming machine (Vistec) used for the thixoforming procedure. The non-dendritic composite billet was placed on the ram, in the middle of the induction coil to ensure uniform reheating. Then the billet was re-heated up to 580°C followed by isothermal holding for 5 minutes to ensure uniform liquid distribution. Besides, isothermal holding also provides sufficient time for microstructural evolution to occur before being forged into the top mould. Figure 3 shows the MWCNT-A356 composite billet of as-cast and as-thixoformed with a height of 70mm and a diameter of 30mm. Table 3 shows the parameters specified for T5 and T6 heat treatments that were applied to the composite billets using a Nabertherm furnace standard.

Table 3. Heat treatment parameters of T5 and T6.

Heat treatment	Solution treatment Temp. (± 10 °C)	Artificial ageing Time (hr)	Artificial ageing Temp. (± 10 °C)	Quenching Time (hr)	Quenching Temp. (°C)
T5	-	-	160	8	-
T6	540	8	160	4	60

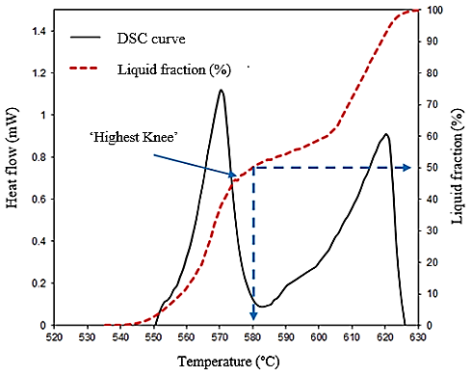

Fig. 1. DSC curve of A356 alloy.

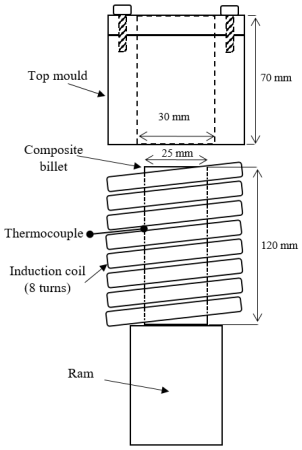

Fig. 2. Schematic diagram of thixoforming machine.

Fig. 3. Composite billet before and after thixoforming process.

2.3. Properties characterizations

A standard metallographic procedure was conducted to the composite at grit sizes of 400, 600, 800 and 1200, polishing with diamond fluid at 6, 3 and 1µm and etching with Keller's solution for 10s. The grain matrix microstructure, size and shape factor were

determined using an optical microscope, Nikon camera and I-Solution DT software, respectively. The average size and shape factor of the non-dendritic matrix were obtained automatically from the software. The phases present in the composites were characterised using X-ray diffraction (XRD), PANalytical system. Meanwhile, the distribution and morphology of the MWCNT at the tensile fractured surfaces were observed using a field-emission scanning electron microscope (FESEM, Hitachi-SU5000). The structural integrity of the MWCNT based on the ratio of defective (D-band, ID) and pristine (G-band, IG), ID/IG was carried out using a Raman spectrometer (UniRAM-Olympus system). Tensile strength and micro-hardness of the composites were determined using an Autograph universal testing machine and a Matsuzawa machine (load = 1kg; dwell time = 10s). The tensile samples were prepared in triplicates based on the ASTM E8M standard to determine the yield strength (YS) at 0.2% strain rate offset, ultimate tensile strength (UTS) and elongation to fracture.

3. Results and Discussion

3.1. Distribution of MWCNT

Figure 4 shows FESEM images of the tensile fracture surfaces of the thixoformed T6 composite at different magnification powers. At a lower magnification power, a well-distributed dimple-liked fracture was noted (as indicated by the arrows in Fig. 4(a)), meanwhile a uniform distribution of MWCNTs were observed at a higher magnification power (as indicated by the arrows in Fig. 4(b)). The integrity of the well-preserved tube structure MWCNT was also confirmed by Raman analysis. Raman spectrum peak intensity ratio, ID/IG (ID at 1350cm^{-1} = 0.7 and IG at 1572cm^{-1} = 0.1) of the received MWCNT was 0.7. On the other hand, the ID/IG of MWCNT in the composite was 0.9. The G-band was shifted to 1590cm^{-1} from 1572cm^{-1} due to the infiltration effect of the MWCNT in the matrix [23]. Therefore, it was only 28.6% (9.0-0.7/0.7*100%) increment in term of structural damage caused by the liquid casting composite processing when comparing the raw MWCNT. In general, this lower ratio of structural damage is difficult to achieve by using the powder processing method. For instance, Chen et al. [6] reported that the ID/IG ratio of raw CNT (1.19) and in the matrix composite (1.46) increased by 46.0% within just an hour of the high energy ball milling process. Moreover, greater structural damage is expected for a longer duration of the ball milling process. In the present study, the MWCNT-A356 composite was successfully produced using the liquid processing method.

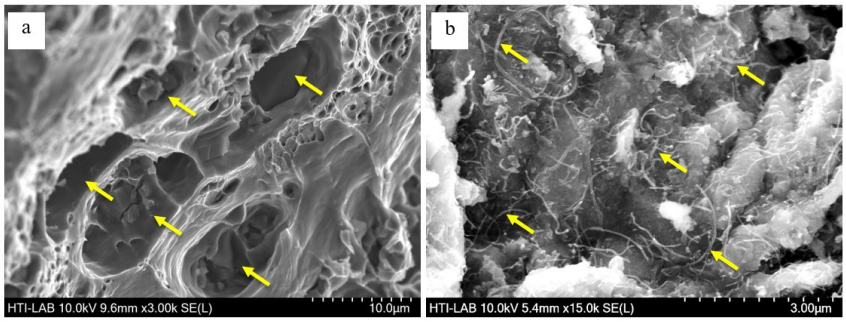

Fig. 4. FESEM images of MWCNT-A356 composite fracture surfaces at (a) 3 000X and (b) 15 000X.

3.2. Microstructures of α-Al and Si

Figure 5 shows microstructures of the composites at four different process conditions. As can be seen in Fig. 5(a), α-Al grain microstructures of the as-cast composite were non-dendritic assuming a spherical shape. The observed microstructure could explain the successful breaking and defragmentation of dendritic arms of the A356 matrix using the mechanical stirring process at the propeller speed of 500 rpm for 10 min. Next, coarse α-Al of thixoformed composite was noted and liquid eutectic in darker areas have reduced as compared with the alloy due to ripening mechanism during isothermal holding above solidus temperature of 580°C or at 50% semi-solid liquid fraction as shown in Fig. 5(b). Microstructures of thixoformed composites at different heat treatments, T5 and T6 are displayed in Figs. 5(c) and 5(d), respectively. There were more eutectic liquid phases and precipitates trapped in α-Al grains in the T5 composite as compared with the T6 composite. The precipitates were mainly composed of Mg_2Si and Al_2Cu that were present in the solid solution during casting. The hardening mechanisms of T5 artificial ageing at a low temperature of 160°C for 8 hours mostly depend on these precipitates. In contrast, the solution treatment (540°C for 8 hours) for T6 composite allowed further dissolution of eutectic and precipitation which resulted in the expansion of α-Al grains size as compared with T5 composite.

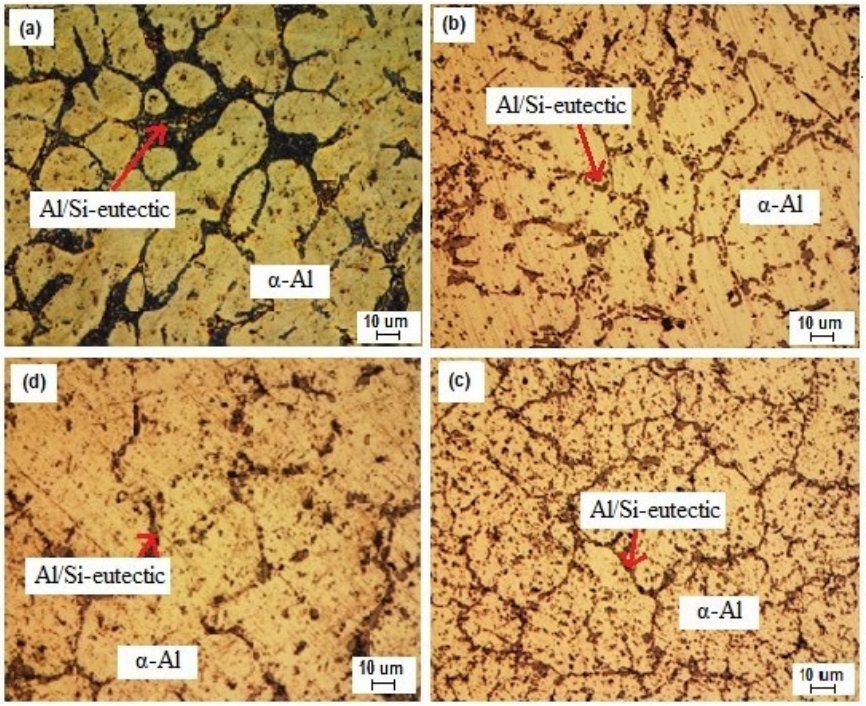

Fig. 5. Microstructures of MWCNT-A356 composites at (a) casting, (b) thixoformed, (c) thixoformed and T5, and (d) thixoformed and T6.

Figure 6 exhibits the average non-dendritic grain sizes and shape factors (SF) of the composites after processing steps. SF is the measure of roundness of the α-

Al grains that was obtained from the I-solution software, with SF equals to 1 indicates a perfect sphere [24-26]. The mechanical stirred of casting A356 alloy grain size and SF obtained were 28.8 ± 24.6μm and 0.523 ± 0.128, respectively as compared to that of the MWCNT-A356 composite which were 23.6 ± 22.8μm and 0.564 ± 0.127μm, respectively. The addition of 0.5 wt.% MWCNT was found to reduce the matrix grain size and improve the shape factor by 22.0% and 7.8%, respectively. The presence of the MWCNT in the matrix functions as an additional shearing force for further defragmentation of dendritic arms to produce a matrix of a finer grain size that could contribute to the matrix Hall-Petch strengthening mechanism [27]. Furthermore, the average size (37.9 ± 11.5μm) and SF (0.545 ± 0.118) of the thixoformed composite increased and get more spherical. Besides coarsening of grains after thixoforming, more uniform shapes were also noted which could cause uniform re-distribution of MWCNT particles in the matrix throughout the grain boundaries. Besides, the disappearance of micro pores present in the matrix might occur during the thixoforming compaction process.

The average grain size of the T6 composite increased to 59.4 ± 37.6μm when compared with 42.9 ± 25.3μm of T5 composite, however, both composites possessed almost equal SF values. According to DSC results (Fig. 1), the T6 composite which was subjected to solution treatment (540°C for 8 hours) had liquid formation in the matrix which further assisted in the coarsening of the grain matrix. Although the T5 composite showed some increment in the grain size, it was insignificant due to the greater size variation noted for T5.

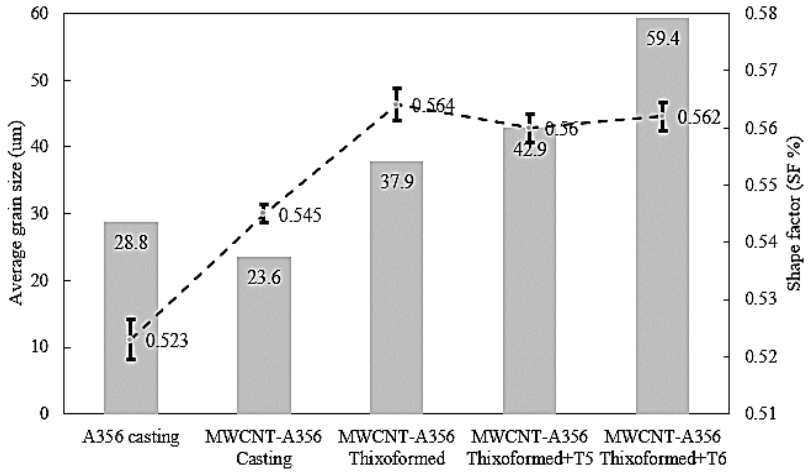

Fig. 6. Average grain sizes and shape factors of alloy and composites.

Figure 7 shows differences in Si microstructure as affected by the different treatment which is another important strengthening factor in the matrix. The β-Si and Si intermetallic phases such as β-Al_5FeSi and β-$Al_8Si_6Mg_3Fe$ assume a needle shape that is inherited via casting. As can be observed in Fig. 7(a), the presence of cracks and weak structure of alloy or composite could be related to high-stress concentration points. Therefore, the transformation of the Si particles into a more spherical shape is beneficial in reducing the stress in the matrix. After the thixoforming process, the Si particles transformed into a more spherical shape

Fig. 7(b) as compared with after casting due to isothermal holding at 580°C. The T6 treatment resulted in the transformation of Si particles into good spherical shape Fig. 7(c) as compared with T5 treatment Fig. 7(d) that was contributed by the higher temperature (540°C) of solution treatment.

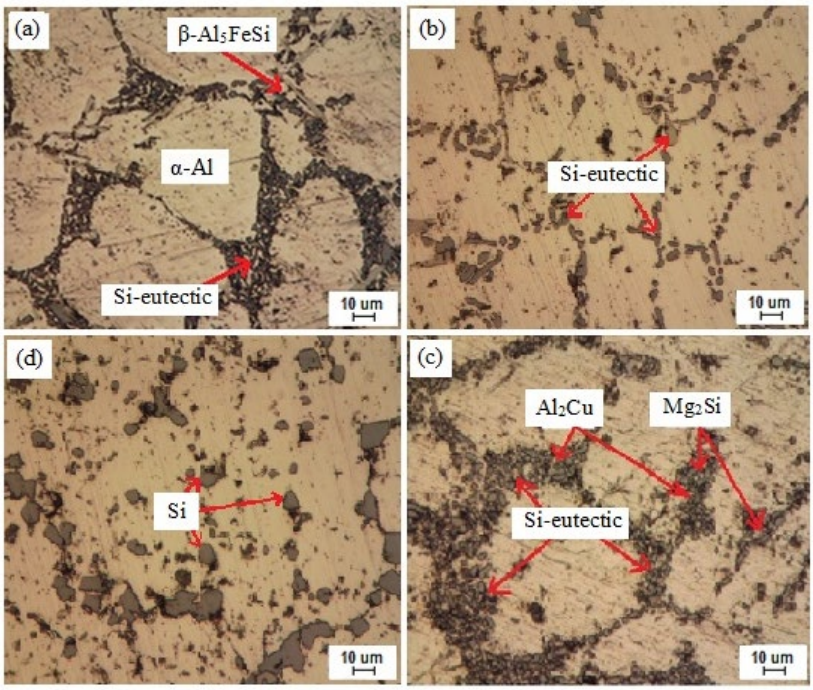

Fig. 7. Microstructures of A356 alloy and MWCNT-A356 composite after (a) casting, (b) thixoformed, (c) thixoformed and T5, and (d) thixoformed and T6.

3.3. Phase precipitation

The major precipitates that formed in as-cast Al-Si-Mg-Cu alloy are α-Al, β-Si, acicular eutectic Si, Mg_2Si and Al_2Cu. The precipitates that consisted of alloying elements can enhance the strength of the alloy by heat treatment. Impurity elements such as Fe and Mn added to the alloy will form intermetallic compounds such as the needle-shaped β-Al_5FeSi and Al_6(Fe, Mn). Besides, these intermetallic compounds create weak points that can initiate a crack in the matrix and deteriorate the mechanical properties of the composite. Figure 8 shows XRD results of precipitates that were present in the composites after T5 and T6 heat treatments. The T5 heat treatment resulted in the precipitation of Mg_2Si and Al_2Cu. Besides, the intermetallic β-Al_5FeSi and π-$Al_8Si_6Mg_3Fe$ were also detected at multiple slip planes as shown in Fig. 8(a). On the contrary, most of the Mg_2Si and Al_2Cu precipitates reduced and dissolved into the atomic level from coarser phases for the T6 composite as shown in Fig. 8(b). The Mg and Cu atoms diffused into the matrix and formed a homogeneous solid solution. Although the intermetallic compounds were still present in the matrix, the intensities were lower as compared with the T5 composite. These conditions led to improvement in the mechanical strength of composite T6 which was higher than T5.

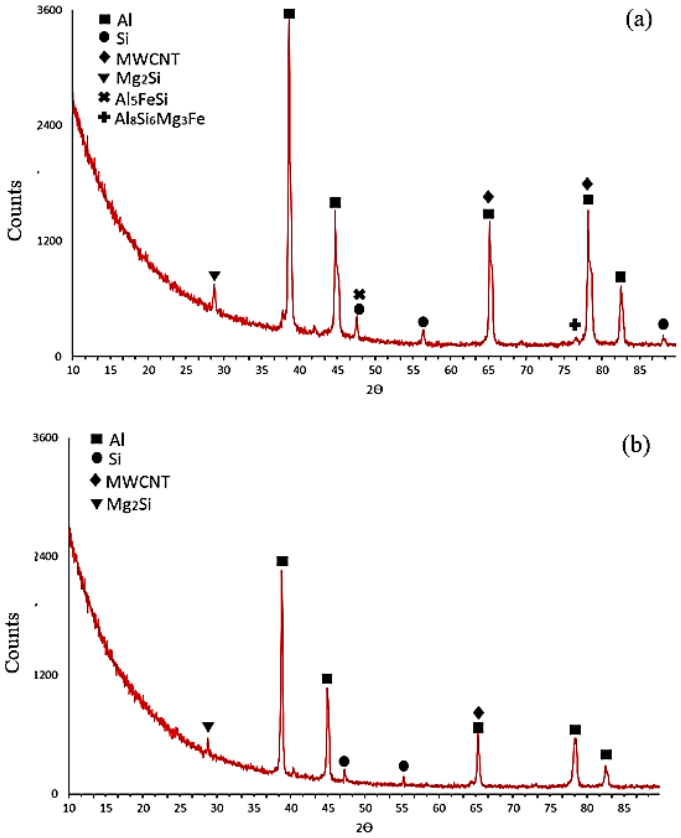

Fig. 8. XRD graph of MWCNT-A356 composites with (a) thixoformed T5, and (b) thixoformed T6.

The XRD findings revealed no detection of interfacial bonding phase of aluminium carbide (Al_4C_3) in both composites which could be due to the smaller amount of Al_4C_3 that has been overshadowed by intensities of major peaks. A substantial amount of Al_4C_3 in the matrix as pinning phase between MWCNT and matrix is crucial to ensure an effective load transfer mechanism [28]. Otherwise, an excessive phase of the nano-rod structure of Al_4C_3 will negatively impact the composite strength.

3.4. Tensile strength

Figure 9 presents the yield strength (YS) and ultimate tensile strength (UTS) of MWCNT-A356 composites after casting, thixoforming, and T5 and T6 heat treatments. The YS and UTS of casting composites increased by 39.8% and 35.5% as compared with casting A356 alloy (YS: 97.52 MPa and UTS: 135.15MPa). The presence of MWCNT in the matrix resulted in a drastic improvement of composites where the better obstruction was created to dislocation movement by several simultaneous strengthening mechanisms. The mechanisms include grain refining, load transfer, Orowan looping and thermal mismatched dislocations [10]. Grain

refining mechanism halts the dislocations by Hall-Petch effect through higher dislocation density and interaction between grain boundaries and smaller average grain size of the composites. Next, the load transfer strengthening mechanism can be defined as the transfer of shear load from matrix to MWCNT via good interfacial bonding of Al_4C_3 phases. The effective load transfer mechanism is often outlined by the bridging and pulled out structures of MWCNT in the matrix as shown in the previous report [21]. Moreover, superior strength and nano-sized inter-particle spacing of MWCNT particles do not allow the dislocations to cut through MWCNT. However, bending around MWCNT and forming dislocation loops before moving to the next particle is called Orowan looping. The mismatching of thermal coefficients between MWCNT and Al can also create a high-density pool of dislocations around MWCNT during solidification. However, since these mechanisms happened simultaneously, it is very difficult to determine the exact percentage of contribution by each mechanism. Thus far, only two related studies were conducted by Park et al. [9] and Liu et al. [29] to calculate the percentage of contribution of each mechanism. Park et al. [9] reported that the YS improved by 68.7% and 31.3% that were attributed to load transfer and thermal mismatch, respectively. Moreover, the load transfer and Orowan looping improved the UTS of MWCNT-Al composite by 51.6% and 30.8%, respectively. Similarly, Liu et al. [29] estimated that the load transfer contributed up to 75.4% and 13.2% which were ascribed to the combined effect of Orowan and thermal dislocations which improved the tensile strength of MWCNT-Al composite. However, these estimations are only possible by assuming the orientations of all MWCNT particles are in the same direction as the final extrusion process of the composites. Otherwise, the estimation through random orientations of the MWCNT in the matrix remains a challenge. Furthermore, the supreme tensile strength of the composites over the alloy also indicates homogeneous distribution of MWCNT and good wettability between MWCNT and matrix.

After the thixoforming process, YS and UTS of composite increased by 49.5% and 37.9%, respectively as compared with the composite after casting. The strength improvement factor in thixoforming is mainly due to the thixotropic behaviour of the semi-solid matrix that allows the non-dendritic matrix movement and coarsening. Furthermore, compacting process at the end of the thixoforming could explain the significant reduction of micro-porosity of the matrix [17]. Thixoforming also permits Si structure transformation to a more spherical shape and uniform MWCNT distribution. The YS and UTS of the thixoformed composite after T6 showed significant improvement by 36.8% and 30.9%, respectively. However, the YS and UTS after T5 almost remained or by slight improvement by 0.7% and 7.2%, respectively. T5 hardening predominantly depends only on the homogenisation of Mg2Si and Al2Cu precipitates in the matrix during the artificial ageing. In contrast, solid solution treatment during T6 allows the dissolution of precipitates, grain coarsening, Si structure transformation and MWCNT to develop stronger hindrance to dislocation movement. Moreover, in general the rate of kinetic ageing precipitations in the composite is much faster than that of the alloy due to high dislocation density. Ageing kinetic during heat treatment is defined as the nucleation rate of precipitation from metastable to more stable states of Guinier-Preston Zone (GPZ) to obstruct dislocation movement. Also, the positive impact of MWCNT in the matrix that led to faster GPZ formation is mainly due to its size in nanometer and a high thermal coefficient difference that generate high dislocations. For micro-size reinforcement particles such as alumina, the GPZ formation was slower and acts as a sink to vacancies and dislocations resulting in a lower composite strength.

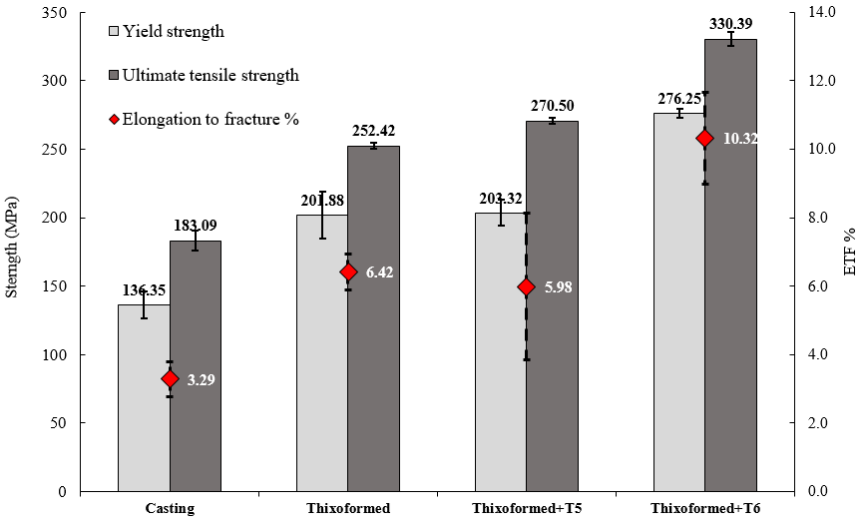

Fig. 9. Tensile strength of MWCNT- A356 composites at different processing stages.

Another important finding is the significant improvement of MWCNT-A356 composite ductility after casting, thixoforming and T6 heat treatment as compared with A356 alloy. Ductility is referred to as the percentage of elongation to fracture (ETF%) of the composite during a tensile test (Fig. 9). The ETF% (> 5%) is a critical requirement for most of the aluminium alloy components in automotive applications such as the engine block, transmission housing, frames, etc., [23, 30]. The ETF% of the composite and A356 alloy obtained from the study were 3.29% and 1.56%, respectively. A high elastic modulus of MWCNT (EMWCNT:1000 GPa) improved the ductility of the composite by 109%, mainly through load transfer from the matrix. The formation of the interfacial layer of Al_4C_3 between the Al matrix and MWCNT helps to prolong plastic deformation during the tensile shearing process. Besides, dimple morphology on the composite fracture surface (Fig. 4(a)) is also evident and indicates ductile fracture. Next, the thixoforming process further increased the composite ductility by another 95% as compared with the as-cast composite due to the elimination of micro-pores in the matrix during microstructure evolution and compaction force. Interestingly, although the tensile strength of the composite increased after T5, the ductility decreased slightly by -6.9%. The finding could be explained by the insufficiency of T5 artificial ageing at 160°C for 8 hours to aid better distribution of MWCNT or generate higher dislocation density around the matrix. In contrast, the ETF% after T6 improved by 60.7% which could be related to the high solution treatment temperature at 540°C for 8 hours. At this temperature, the onset of dissolution of intermetallic compounds was noted, besides spheriodization of Si and further coarsening of the matrix that has a positive impact on the composite strength. Besides, during quenching of T6, higher dislocation density was generated in the matrix due to thermal mismatch between MWCNT and Al which acts as stronger pinning to dislocation movement.

4. Conclusions

The effects of T5 and T6 heat treatments on mechanical properties and microstructure evolution of MWCNT-A356 composites are discussed in the present study. The composites were prepared using a liquid casting technique with the use of Mg power as the wettability agent and mechanical stirring to distribute MWCNT reinforcements and disturbed the formation of dendritic matrix microstructures. The composites were also re-heated to semi-solid state of thixoforming process up to 580°C upon compaction. Thus, the grain size of non-dendritic microstructure increases up to 60% after thixoforming due to coarsening and fusion of α-Al grains. These grains have expanded by 13% and 57% after T5 and T6 heat treatments, respectively. The significant grains expansion after T6 was due to the starting point of α-Al liquid formation during isothermal holding solution treatment temperature at 540°C.

Overall, T6 heat treatment on the thixoformed composite showed superior strength and ductility as compared with the thixoformed and T5. The UTS and ETF% of thixoformed T6 and T5 increase to (330.3 MPa and 10.3%) and (270.5 MPa and 5.98%), respectively as compared with after thixoformed (252.4 MPa and 6.42%). The tensile strength of these thixoformed T6 and T5 are significantly higher compared with the UTS values of 0.5 wt.% MWCNT-A356 composites obtained by Elshalakany et al. [31] and Pyo et al. [32] of 250 MPa and 265 MPa, respectively. In artificial ageing of T5, precipitation of Mg_2Si and Al_2Cu was the only strengthening mechanism. Although the tensile strength improved, the ductility decreased slightly. However, the solution treatment and quenching of T6 resulted in the dissolution of intermetallic precipitates, enhancement of MWCNT distribution and generation of higher dislocation density that led to superior strength and ductility of the composites.

Two key factors of successful MWCNT-A356 composite development include homogenous distribution and minimal structural damage of MWCNT in the A356 matrix using the liquid casting technique. Overall strength and ductility of the composites improved tremendously as compared to the A356 alloy. The MWCNT strengthening mechanisms are based on grain refinement, load transfer, Orowan looping and thermal mismatch dislocations. For the composite, matrix grain refining was obtained by the additional shearing forces provided by MWCNT to break the dendritic arm formation during stirring. Furthermore, an interfacial layer of Al_4C_3 acted as the pinning phase between MWCNT and Al matrix. Meanwhile, the Orowan and thermal mismatch created a higher density of dislocations in the matrix that obstructed the movement of further dislocations that helps to enhance the composite strength.

Simple liquid casting processing of MWCNT-A356 composite is the main advantage for automotive parts production. Although the composite ductility of T5 is lower than T6, it is still above 5% (ETF%) and may satisfy the requirements of certain components in related fields with a cost-effective heat-treatment process. Therefore, the T6 heat treatment can be further optimised to meet the cost-saving demand in the industry.

Acknowledgments

The authors would like to extend a special thank you to the Centre for Research and Innovation Management (CRIM) and Fakulti Teknologi Kejuruteraan Mekanikal dan Pembuatan, Universiti Teknikal Malaysia, Melaka.

References

1. Grosselle, F.; Timelli, G.; and Bonollo, F. (2010). Doe applied to microstructural and mechanical properties of Al-Si-Cu-Mg casting alloys for automotive applications. *Materials Science and Engineering: A*, 527(15), 3536-3545.
2. Singh, J.; and Chauhan, A. (2015). Characterization of hybrid aluminum matrix composites for advanced applications - A review. *Journal of Materials Research and Technology*, 5(2), 159-169.
3. Mallick. P.K. (2012). *Advanced materials for automotive applications: an overview*. Woodhead Publishing Limited.
4. Möller, H.; Govender, G.; and Stumpf, W. E. (2010). Application of shortened heat treatment cycles on A356 automotive brake calipers with respective globular and dendritic microstructures. *Transactions of Nonferrous Metal Society of China*, 20(9), 1780-1785.
5. Erzi, E.; Gürsoy, O.; Colak, M.; and Dispinar, D. (2019). Determination of acceptable quality limit for casting of A356 aluminium alloy: Supplier' s quality index (SQI). *Metals*, 9(9), 957.
6. Chen, B.; Li, S.; Imai, H.; Jia, L.; Umeda, J.; Takahashi, M.; and Kondoh, K. (2015). An approach for homogeneous carbon nanotube dispersion in Al matrix composites. *Materials & Design*, 72, 1-8.
7. Hashim, J.; Looney, L.; and Hashmi, M.S.J. (1999). Metal matrix composites: production by the stir casting method. *Journal of Materials Processing Technology*, 92-93, 1-7.
8. Boostani, A.F.; Yazdani, S.; Mousavian, R.T.; Tahamtan, S.; Khosroshahi, R.A.; Wei, D.; Brabazon, D.; Xu, J.Z.; Zhang, X.M.; and Jiang, Z.Y. (2015). Strengthening mechanisms of graphene sheets in aluminium matrix nanocomposites. *Materials & Design*, 88, 983-989.
9. Park, J.G.; Keum, D.H.; and Lee, Y.H. (2015). Strengthening mechanisms in carbon nanotube-reinforced aluminum composites. *Carbon*, 95, 690-698.
10. Mokdad, F.; Chen, D.L.; Liu, Y.Z.; Xiao, B.L.; Ni, D.R.; and Ma, Z.Y. (2016). Deformation and strengthening mechanisms of a carbon nanotube reinforced aluminum composite. *Carbon*, 104, 64-77.
11. Chen, B.; Shen, J.; Ye, X.; Imai, H.; Umeda, J.; Takahashi, M.; Kondoh, K. (2017). Solid-state interfacial reaction and load transfer efficiency in carbon nanotubes (CNTs)-reinforced aluminum matrix composites. *Carbon*, 114, 198-208.
12. Hanizam, H.; Salleh, M.S.; Omar, M.Z.; Sulong, A.B.; Yahaya, S.H.; and Siswanto, N. (2019). Effect of magnesium surfactant on wettability of carbon nanotube in A356 alloy composite. *Journal of Advanced Manufacturing Technology*, 13(2), 1-11.
13. Chen, B.; Shen, J.; Ye, X.; Jia, L.; Imai, H.; Umeda, J.; Takahashi, M.; and Kondoh, K. (2017). Length effect of carbon nanotubes on the strengthening mechanisms in metal matrix composites. *Acta Materialia*, 140, 317-325.
14. Esawi, A.M.K.; Morsi, K.; Sayed, A.; Taher, M.; and Lanka, S. (2011). The influence of carbon nanotube (CNT) morphology and diameter on the

processing and properties of CNT-reinforced aluminium composites. *Composites Part A: Applied Science and Manufacturing*, 42(3), 234-243.

15. Hanizam, H.; Salleh, M.S.; Omar, M.Z.; Sulong, A.B.; and Arif. M.A.M. (2020). Effects of hybrid processing on microstructural and mechanical properties of thixoformed aluminum matrix composite. *Journal of Alloys and Compounds*, 836, 155378.
16. Cavaliere, P.; Cerri, E.; and Leo, P. (2005). Effect of heat treatments on mechanical properties and damage evolution of thixoformed aluminium alloys. *Materials Characterization*, 55(1), 35-42.
17. Salleh, M.S.; Omar, M.Z.; Syarif, J.; Alhawari, K.S.; and Mohammed, M.N. (2014). The effects of Cu content on microstructure and mechanical properties of thixoformed A319 aluminium alloys. *Applied Mechanics and Materials*, 548-549, 237-241.
18. Birol, Y. (2008). Cooling slope casting and thixoforming of hypereutectic A390 alloy. *Journal of Materials Processing Technology*, 207(1-3), 200-203.
19. Peng, J.H.; Tang, X.L.; He, J.T.; and Xu, D.Y. (2011). Effect of heat treatment on microstructure and tensile properties of A356 alloys. *Transactions of Nonferrous Metal Society of China*, 21(9), 1950-1956.
20. Lasa, L.; and Rodriguez-Ibabe, J.M. (2004). Evolution of the main intermetallic phases in Al-Si-Cu-Mg casting alloys during solution treatment. *Journal of Materials Science*, 39(4), 1343-1355.
21. Hanizam, H.; Salleh, M.S.; Omar, M.Z.; and Sulong, A.B. (2019). Optimisation of mechanical stir casting parameters for fabrication of carbon nanotubes-aluminium alloy composite through Taguchi method. *Journal of Materials Research and Technology*, 8(2), 2223-2231.
22. Hanizam, H.; Salleh, M.S.; Omar, M.Z.; and Sulong, A.B. (2019). Effects of mechanical stirring and short heat treatment on thixoformed of carbon nanotube aluminium alloy composite. *Journal of Alloys and Compounds*, 788, 83-90.
23. Chen, B.; Kondoh, K.; Imai, H.; Umeda, J.; and Takahashi, M. (2016). Simultaneously enhancing strength and ductility of carbon nanotube/aluminum composites by improving bonding conditions. *Scripta Materialia*, 113, 158-162.
24. Arrabal, R.; Mingo, B.; Pardo, A.; Mohedano, M.; Matykina, E.; and Rodríguez, I. (2013). Pitting corrosion of rheocast A356 aluminium alloy in 3.5wt.% NaCl solution. *Corrosion Science*, 73, 342-355.
25. Taghavi, F.; Saghafian, H.; and Kharrazi, Y.H.K. (2009). Study on the ability of mechanical vibration for the production of thixotropic microstructure in A356 aluminum alloy. *Materials & Design*, 30 (1), 115-121.
26. Salleh, M.S.; Omar, M.Z.; Syarif, J.; and Mohammed, M.N. (2013). An overview of semisolid processing of aluminium alloys. *Materials Science*, Volume 2013, Article ID 679820, 1-9.
27. Liu, Z.; Yan, H.; Tu, K.; and Xiong, J.J. (2022). Microstructure and tribological properties of Al 7075-TiO2@CNTs composites under T6 treatment. *Vacuum* 199, 110949.
28. Liu, X.; Li, C.; Eckert, J.; Prashanth, K.G.; Renk, O.; Teng, L.; Liu, Y.; Bao, R.; Tao. J.; Shen, T.; Yi, J. (2017). Microstructure evolution and mechanical properties of carbon nanotubes reinforced Al matrix composites. *Materials Characterization*, 133, 122-132.

29. Liu, X.; Li, J.; Liu, E.; Li, Q.; He, C.; Shi, C.; and Zhao, N. (2018). Effectively reinforced load transfer and fracture elongation by forming Al4C3 for in-situ synthesizing carbon nanotube reinforced Al matrix composites. *Materials Science & Engineering: A*, 718, 182-189.
30. Zhang, P.; Li, Z.; Liu, B.; and Ding, W. (2017). Tensile properties and deformation behaviors of a new aluminum alloy for high pressure die casting. *Journal of Materials Science & Technology*, 33(4), 367-378.
31. Elshalakany, A.B.; Osman, T.A.; Khattab, A.; Azzam, B; and Zaki, M. (2014). Microstructure and mechanical properties of MWCNTs reinforced A356 aluminum alloys cast nanocomposites fabricated by using a combination of rheocasting and squeeze casting techniques. *Journal of Nanomaterials*, Volume 2014, Article ID 386370,1-14.
32. So, K.P.; Jeong, J.C.; Park, J.G.; Park, H.K.; Choi, Y.H.; Noh, D.H.; Keum, D.H.; Jeong, H.Y.; Biswas, C.; Hong, C.H.; and Lee, Y.H. (2013). SiC formation on carbon nanotube surface for improving wettability with aluminum. *Composites Science & Technology*, 74, 6-13.